

# Structure of a neutral exopolysaccharide produced by *Lactobacillus delbrueckii* ssp. *bulgaricus* LBB.B26

Inmaculada Sánchez-Medina,<sup>a</sup> Gerrit J. Gerwig,<sup>a</sup> Zoltan L. Urshev<sup>b</sup>  
and Johannes P. Kamerling<sup>a,\*</sup>

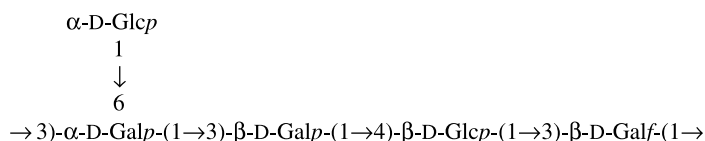
<sup>a</sup>*Bijvoet Center, Department of Bio-Organic Chemistry, Utrecht University, Padualaan 8, NL-3584 CH Utrecht, The Netherlands*

<sup>b</sup>*LB Bulgaricum Plc., R&D Center, 12A Malashevska str., Sofia 1202, Bulgaria*

Received 13 April 2007; received in revised form 6 June 2007; accepted 11 June 2007

Available online 20 June 2007

**Abstract**—The neutral exopolysaccharide produced by *Lactobacillus delbrueckii* ssp. *bulgaricus* LBB.B26 in skimmed milk was found to be composed of D-glucose and D-galactose in a molar ratio of 2:3. Linkage analysis and 1D/2D NMR (<sup>1</sup>H and <sup>13</sup>C) studies performed on the native polysaccharide, and on an oligosaccharide obtained from a partial acid hydrolysate of the native polysaccharide, showed the polysaccharide to consist of branched pentasaccharide repeating units with the following structure:



© 2007 Elsevier Ltd. All rights reserved.

**Keywords:** *Lactobacillus delbrueckii* ssp. *bulgaricus*; Exopolysaccharide; Lactic acid bacteria; Structural analysis; NMR spectroscopy; Mass spectrometry

## 1. Introduction

Microbial exopolysaccharides (EPSs) are widely used in the food industry as viscosifying, stabilizing, gelling, or emulsifying agents, due to their characteristic physical and rheological properties.<sup>1–3</sup> In this context, a growing interest has developed in the use of EPSs produced by lactic acid bacteria which carry the GRAS (Generally Recognized As Safe) status. To gain a better insight into the relationship between the structures of EPSs and their physical/rheological properties, structural studies are currently performed on EPSs produced by different species of lactic acid bacteria, such as *Lactobacillus*, *Lactococcus*, and *Streptococcus* species.

*Lactobacillus delbrueckii* ssp. *bulgaricus* strains are usually applied in combination with *Streptococcus thermophilus* strains as commercial yoghurt starters. Over the years, several EPSs produced by *Lb. delbrueckii* ssp. *bulgaricus* have been characterized, being mainly composed of Glc and Gal<sup>4–7</sup> or of Glc, Gal, and Rha.<sup>8–11</sup>

Here, we report on the structural determination of the neutral EPS produced by *Lb. delbrueckii* ssp. *bulgaricus* LBB.B26 in skimmed milk.

## 2. Results and discussion

### 2.1. Isolation, purification, and composition of the exopolysaccharide

The neutral EPS produced by *Lb. delbrueckii* ssp. *bulgaricus* LBB.B26 was isolated via absolute ethanol precipi-

\* Corresponding author. Tel.: +31 30 253 34 79; fax: +31 30 254 09 80; e-mail: [j.p.kamerling@chem.uu.nl](mailto:j.p.kamerling@chem.uu.nl)

tation of the trichloroacetic acid-treated culture medium, and further purified by anion-exchange chromatography on DEAE-Trisacryl Plus M. Its average molecular mass was determined by gel filtration chromatography on Sephacryl S-400 HR to be  $1.3 \times 10^6$  Da.

Quantitative monosaccharide analysis, including absolute configuration determination, of the EPS revealed D-Glc and D-Gal in a molar ratio of 1.0:1.8. Methylation analysis (Table 1) showed the presence of terminal Glcp, 4-substituted Glcp (or 5-substituted Glcf), 3-substituted Galf, 3-substituted Galp, and 3,6-disubstituted Galp in a molar ratio of 1.0:1.1:1.0:1.4:0.8, suggesting a branched, pentameric repeating unit. According to NMR experiments (vide infra), the monosubstituted Glc residue is in the pyranose ring form.

The 1D  $^1\text{H}$  NMR spectrum of the EPS (Fig. 1) showed five major signals in the anomeric region ( $\delta$  4.5–5.5), supporting a pentasaccharide repeating unit. The monosaccharide residues in the EPS were arbitrarily named from A to E, according to decreasing chemical shift values of their anomeric protons. Taking into account the chemi-

cal shift as well as the value of the coupling constant for each anomeric signal, residue A ( $\delta$  5.245,  $^3J_{1,2} < 2$  Hz) was identified as furanose ring with  $\beta$  configuration (vide infra), residue C ( $\delta$  4.977,  $^3J_{1,2}$  3.4 Hz) as pyranose ring with  $\alpha$  configuration, and residues D ( $\delta$  4.682,  $^3J_{1,2}$  7.3 Hz) and E ( $\delta$  4.537,  $^3J_{1,2}$  7.2 Hz) as pyranose rings with  $\beta$  configuration. Due to the shape of the signal, the value of  $^3J_{1,2}$  for residue B ( $\delta$  5.165) could not be determined exactly, but considering the chemical shift of the anomeric proton, it was assigned as pyranose ring with  $\alpha$  configuration (vide infra).

## 2.2. Partial acid hydrolysis and analysis of the pentasaccharide repeating unit

Partial acid hydrolysis of the native EPS yielded a complex mixture of oligosaccharides, which was fractionated on Bio-Gel P-4, affording fractions 1–4 (Fig. 2). As checked by 1D  $^1\text{H}$  NMR and TLC analyses (data not shown), fraction 1 contained non-degraded EPS and high-molecular-mass fragments, fraction 2 a mixture of

**Table 1.** Methylation analysis data of *Lactobacillus delbrueckii* ssp. *bulgaricus* LBB.B26 neutral EPS and oligosaccharide 3

Partially methylated alditol acetate	$T_R^a$	Structural feature	Molar ratio EPS <sup>b</sup>	Molar ratio 3 <sup>b</sup>
2,3,4,6-Tetra- <i>O</i> -methyl-1,5-di- <i>O</i> -acetylglucitol-1- <i>d</i>	1.00	Glcp-(1→	1.0	1.2
2,5,6-Tri- <i>O</i> -methyl-1,3,4-tri- <i>O</i> -acetylgalactitol-1- <i>d</i>	1.18	→3)-Galp-(1→	1.0	—
2,3,6-Tri- <i>O</i> -methyl-1,4,5-tri- <i>O</i> -acetylglucitol-1- <i>d</i>	1.21	→4)-Glcp-(1→	1.1	0.9
2,4,6-Tri- <i>O</i> -methyl-1,3,5-tri- <i>O</i> -acetylgalactitol-1- <i>d</i>	1.23	→3)-Galp-(1→	1.4	1.7
2,4-Di- <i>O</i> -methyl-1,3,5,6-tetra- <i>O</i> -acetylgalactitol-1- <i>d</i>	1.51	→3,6)-Galp-(1→	0.8	—
2,3,4-Tri- <i>O</i> -methyl-1,5,6-tri- <i>O</i> -acetylgalactitol-1- <i>d</i>	1.32	→6)-Galp-(1→	—	1.0

<sup>a</sup> GLC retention times relative to 2,3,4,6-tetra-*O*-methyl-1,5-di-*O*-acetylglucitol-1-*d* on EC-1.

<sup>b</sup> Calculated from peak areas, not corrected by response factors.

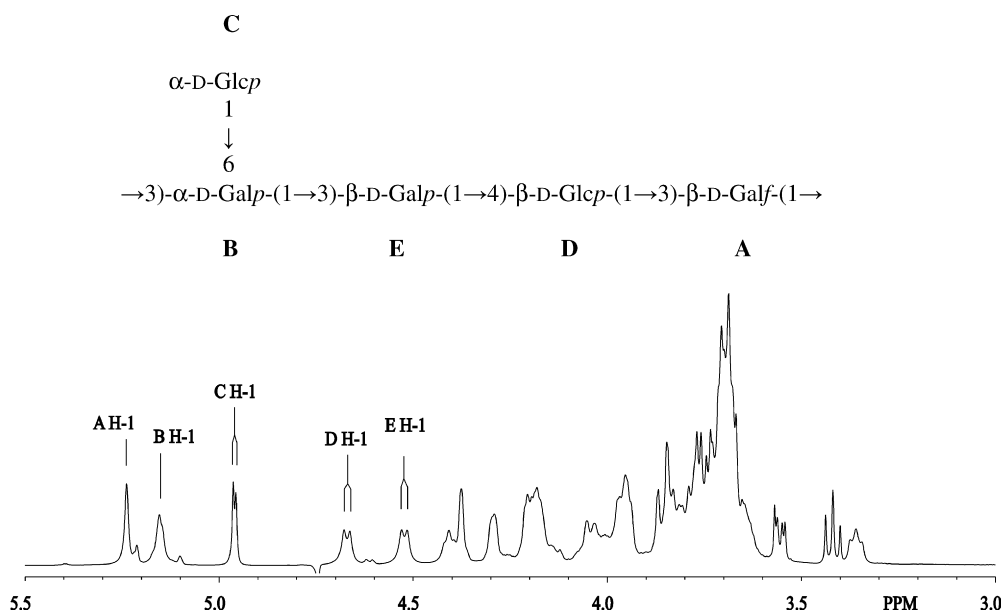


**Figure 1.** 500-MHz 1D  $^1\text{H}$  NMR spectrum of the neutral EPS produced by *Lactobacillus delbrueckii* ssp. *bulgaricus* LBB.B26, recorded in  $\text{D}_2\text{O}$  at 27 °C.

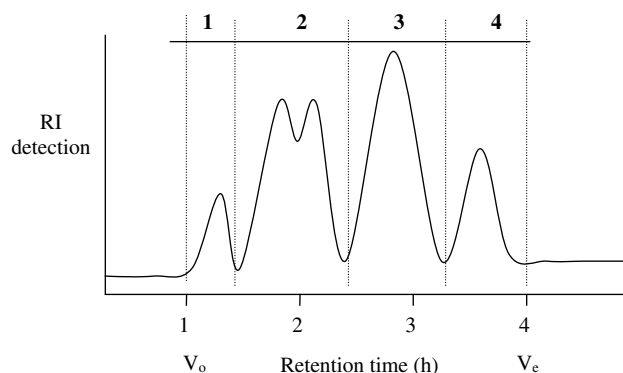


**Figure 2.** Bio-Gel P-4 elution profile of partially acid hydrolyzed EPS, monitored by refractive index detection.

oligosaccharides larger than pentasaccharides, fraction **3** a pure pentasaccharide, and fraction **4** a mixture of trisaccharides. In the context of this study, only fraction **3** has been analyzed in detail.

The MALDI-TOF mass spectrum of fraction **3** showed a single  $[M+Na]^+$  pseudomolecular ion at  $m/z$  851.6, corresponding with Hex<sub>5</sub>. Monosaccharide analysis gave a composition of D-Glc and D-Gal in a molar ratio of 2:3. Methylation analysis (Table 1) gave evidence for the occurrence of terminal Glcp, 4-substituted Glcp, 3-substituted Galp, and 6-substituted Galp in a molar ratio of 1.2:0.9:1.7:1.0, suggesting a linear pentasaccharide structure. In view of the established oligosaccharide structure (vide infra), it is clear that, if  $\beta$ -elimination had occurred (peeling, due to the 3-substituted reducing Gal unit), it was only to a small extent.

In the 1D  $^1H$  NMR spectrum of **3** (Fig. 3), six anomeric signals were found at  $\delta$  5.290 (residue A $\alpha$ ,  $^3J_{1,2}$  3.0 Hz),  $\delta$  5.146 (residue B,  $^3J_{1,2}$  3.6 Hz),  $\delta$  4.979

(residue C,  $^3J_{1,2}$  3.6 Hz),  $\delta$  4.720/4.704 (residue D $\alpha$ /D $\beta$ ,  $^3J_{1,2}$  7.0 Hz),  $\delta$  4.641 (residue A $\beta$ ,  $^3J_{1,2}$  7.9 Hz), and  $\delta$  4.541 (residue E,  $^3J_{1,2}$  7.3 Hz). Considering the chemical shifts and the coupling constants observed, residues B and C were identified as pyranose ring forms with  $\alpha$  configuration, while residues D and E were assigned as pyranose ring forms with  $\beta$  configuration. Residue A $\alpha$ /A $\beta$  represents the reducing end of the oligosaccharide. The twinning observed for the anomeric signal of residue D is due to the influence of the  $\alpha/\beta$  configuration of residue A.

The  $^1H$  chemical shifts of oligosaccharide **3** (Table 2) were assigned by means of 2D TOCSY (mixing times, 40–150 ms), NOESY (mixing time, 1 s), and  $^1H$ – $^{13}C$  HSQC experiments. The TOCSY spectrum (150 ms) of oligosaccharide **3** is shown in Figure 4, together with the NOESY spectrum. Starting points for the interpretation of the spectra were the anomeric signals of residues A $\alpha$ –E. Comparison of TOCSY spectra with increasing mixing times allowed the assignment of the sequential order of the chemical shifts belonging to the same spin system.

The TOCSY A $\alpha$  H-1 track ( $\delta$  5.290) showed cross-peaks with A $\alpha$  H-2,3,4. On the A $\alpha$  H-4 track the cross-peak with A $\alpha$  H-5 was found, and on the A $\alpha$  H-5 track the resonances for A $\alpha$  H-6a,b. The TOCSY B H-1 track ( $\delta$  5.146) allowed the observation of cross-peaks with B H-2,3,4,5; via the B H-5 track the cross-peaks with B H-6a and 6b were found (confirmed by  $^1H$ – $^{13}C$  HSQC). On the TOCSY C H-1 track ( $\delta$  4.979), resonances for C H-2,3,4,5,6a,6b were observed (confirmed by  $^1H$ – $^{13}C$  HSQC). Following the TOCSY D H-1 track ( $\delta$  4.720/4.704), the cross-peaks with D H-2,3,4,5,6b were detected (confirmed by  $^1H$ – $^{13}C$  HSQC), whereas the D H-6b track revealed the D H-6a resonance (confirmed

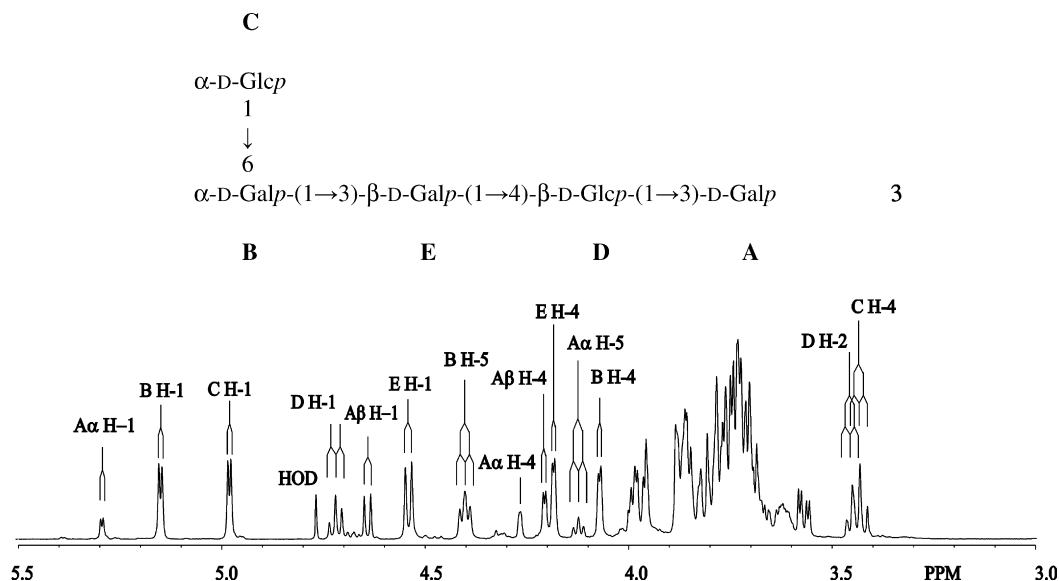


**Figure 3.** 500-MHz 1D  $^1H$  NMR spectrum of oligosaccharide **3**, recorded in D<sub>2</sub>O at 27 °C.

**Table 2.**  $^1\text{H}$  and  $^{13}\text{C}$  NMR chemical shifts<sup>a</sup> of EPS and oligosaccharide **3**, recorded in  $\text{D}_2\text{O}$  at 27 °C

Residue	Proton	EPS	<b>3</b>	Carbon	EPS	<b>3</b>
<b>A</b> →3)-β-D-Galp-(1→	H-1	5.245 (<2)	—	C-1	110.5 (177)	—
	H-2	4.39	—	C-2	80.9	—
	H-3	4.31	—	C-3	85.6	—
	H-4	4.21	—	C-4	83.2	—
	H-5	3.97	—	C-5	71.5	—
	H-6a	3.69	—	C-6	63.8	—
	H-6b	3.69	—			
<b>B</b> →3,6)-α-D-Galp-(1→	H-1	5.165 (n.d.)	—	C-1	96.5 (173)	—
	H-2	3.98	—	C-2	68.2	—
	H-3	4.06	—	C-3	78.0	—
	H-4	4.19	—	C-4	70.2	—
	H-5	4.27	—	C-5	76.4	—
	H-6a	3.84	—	C-6	67.0	—
	H-6b	3.71	—			
<b>C</b> α-D-Glcp-(1→	H-1	4.977 (3.4)	4.979 (3.6)	C-1	99.0 (173)	98.9 (172)
	H-2	3.56	3.57	C-2	72.3	72.4
	H-3	3.69	3.71	C-3	74.4	74.2
	H-4	3.43	3.436	C-4	70.6	70.5
	H-5	3.71	3.72	C-5	72.9	72.9
	H-6a	3.87	3.87	C-6	61.5	61.6
	H-6b	3.77	3.77			
<b>D</b> →4)-β-D-Glcp-(1→	H-1	4.682 (7.3)	4.720/4.704 (7.0)	C-1	102.9 (163)	104.6 (162)
	H-2	3.37	3.449	C-2	73.7	74.1
	H-3	3.70	3.70	C-3	75.3	75.2
	H-4	3.71	3.73	C-4	79.4	79.2
	H-5	3.65	3.62	C-5	75.8	75.6
	H-6a	4.02	3.97	C-6	61.0	60.9
	H-6b	3.85	3.87			
<b>E</b> →3)-β-D-Galp-(1→	H-1	4.537 (7.2)	4.541 (7.3)	C-1	103.9 (161)	103.8 (164)
	H-2	3.70	3.69	C-2	70.6	70.5
	H-3	3.79	3.78	C-3	78.3	78.2
	H-4	4.18	4.185	C-4	65.9	65.8
	H-5	3.74	3.74	C-5	76.1	76.1
	H-6a	3.79	3.82	C-6	62.1	62.0
	H-6b	3.79	3.82			
<b>Aα</b> →3)-α-D-Galp	H-1	—	5.290 (3.0)	C-1	—	93.2 (172)
	H-2	—	3.99	C-2	—	68.4
	H-3	—	3.99	C-3	—	80.6
	H-4	—	4.265	C-4	—	69.9
	H-5	—	4.123	C-5	—	71.1
	H-6a	—	3.78	C-6	—	62.0
	H-6b	—	3.78			
<b>Aβ</b> →3)-β-D-Galp	H-1	—	4.641 (7.9)	C-1	—	97.2 (n.d.)
	H-2	—	3.66	C-2	—	71.9
	H-3	—	3.81	C-3	—	83.7
	H-4	—	4.206	C-4	—	69.4
	H-5	—	3.74	C-5	—	75.8
	H-6a	—	3.78	C-6	—	62.0
	H-6b	—	3.78			
<b>B</b> →6)-α-D-Galp-(1→	H-1	—	5.146 (3.6)	C-1	—	96.5 (172)
	H-2	—	3.88	C-2	—	69.3
	H-3	—	3.97	C-3	—	70.3
	H-4	—	4.072	C-4	—	70.3
	H-5	—	4.402	C-5	—	69.8
	H-6a	—	3.87	C-6	—	67.2
	H-6b	—	3.73			

<sup>3</sup> $J_{1,2}$  and  $^1J_{\text{C-1,H-1}}$  coupling constants are included in parentheses.<sup>a</sup> In ppm relative to the signal of internal acetone at  $\delta$  2.225 for  $^1\text{H}$ , and in ppm relative to the signal of external [ $1\text{-}^{13}\text{C}$ ] glucose ( $\delta_{\text{C-1}}$  92.9) for  $^{13}\text{C}$ .

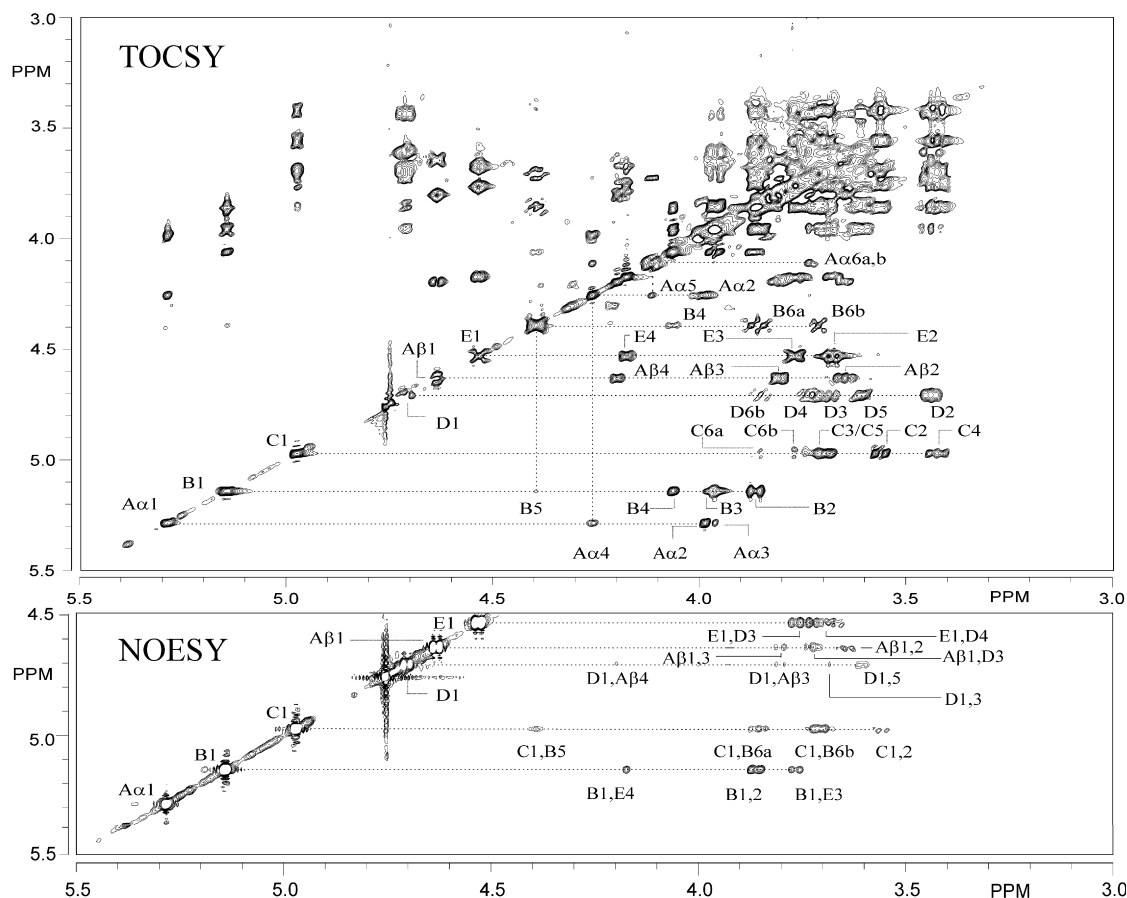


**Figure 4.** 2D TOCSY (mixing time, 150 ms) and NOESY (mixing time, 1 s) spectra of oligosaccharide **3**, recorded in D<sub>2</sub>O at 27 °C. Cross-peaks belonging to the same scalar-coupling network are indicated near a dotted line starting from the corresponding diagonal peaks; TOCSY: B1 corresponds to the diagonal peak of residue **B** H-1; B2 refers to a cross-peak between **B** H-1 and **B** H-2, etc.; NOESY: B1 corresponds to the diagonal peak of residue **B** H-1; B1,2 refers to an intra-residue cross-peak between **B** H-1 and **B** H-2, and B1,E4 indicates an inter-residue connectivity between **B** H-1 and **E** H-4, etc.

by <sup>1</sup>H–<sup>13</sup>C HSQC). The TOCSY Aβ H-1 track (δ 4.641) showed cross-peaks with Aβ H-2,3,4, and the chemical shifts of Aβ H-5 and H-6a,b were deduced from <sup>1</sup>H–<sup>13</sup>C HSQC experiments. Finally, on the TOCSY E H-1 track (δ 4.541) cross-peaks with E H-2,3,4 were found; the resonances for E H-5 and H-6a,b followed from <sup>1</sup>H–<sup>13</sup>C HSQC experiments.

The typical H-2,3,4 spin systems seen on the TOCSY H-1 tracks of residues **A**, **B**, and **E**, with downfield chemical shift values for their H-4 signals (<sup>3</sup>J<sub>3,4</sub> 3 Hz, <sup>3</sup>J<sub>4,5</sub> < 1 Hz), indicated a *galacto*-configuration for each of these residues; the TOCSY results of residues **C** and **D** are in agreement with a *gluco*-configuration.

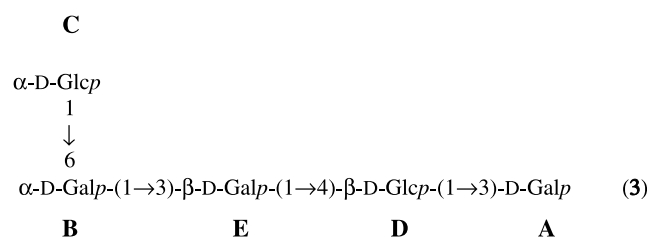
The <sup>13</sup>C chemical shifts of oligosaccharide **3** were assigned (Table 2) by using 2D <sup>1</sup>H–<sup>13</sup>C HSQC experiments, whereas a 2D <sup>1</sup>H–<sup>13</sup>C HMBC spectrum revealed the <sup>1</sup>J<sub>C-1,H-1</sub> coupling constants. Based on their C-1 chemical shifts and <sup>1</sup>J<sub>C-1,H-1</sub> coupling constants, residues **B** (Gal; δ 96.5; 172 Hz) and **C** (Glc; δ 98.9; 172 Hz) occur in α-pyranosyl form, and residues **D** (Glc; δ 104.6; 162 Hz) and **E** (Gal; δ 103.8; 164 Hz) in β-pyranosyl form.<sup>12</sup>

Taking into account published <sup>13</sup>C chemical shift data of (methyl) aldoses,<sup>13</sup> and the methylation analysis data of oligosaccharide **3**, residue **C** could be identified as the terminal α-Glcp residue. The downfield chemical shifts of Aα C-3 (δ<sub>C-3</sub> 80.6; α-D-Galp, δ<sub>C-3</sub> 70.2) and Aβ C-3 (δ<sub>C-3</sub> 83.7; β-D-Galp, δ<sub>C-3</sub> 73.8) demonstrated residue **A** to represent the 3-substituted Galp residue. In a similar way, the downfield chemical shift of **B** C-6 (δ<sub>C-6</sub> 67.2; α-D-Galp1Me, δ<sub>C-6</sub> 62.2) allowed the identification of residue **B** as 6-substituted α-Galp, the downfield chemical shift of **D** C-4 (δ<sub>C-4</sub> 79.2; β-D-Glcp1Me, δ<sub>C-4</sub> 70.6) residue **D** as 4-substituted β-Glcp, and the downfield chemical shift of **E** C-3 (δ<sub>C-3</sub> 78.2; β-D-Galp1Me, δ<sub>C-3</sub> 73.8) residue **E** as 3-substituted β-Galp.

Finally, the determination of the sequence of the monosaccharide residues within the pentasaccharide was established through the assignment of the inter-residue cross-peaks in the 2D NOESY spectrum (Fig. 4). On the NOESY **C** H-1 track, inter-residue cross-peaks with **B** H-6a,6b were found, indicating a C(1→6)**B** linkage. The NOE cross-peaks between **B** H-1 and **E** H-3,4 gave evidence for a linkage between **B** and **E**, and in

view of the methylation analysis/ $^{13}\text{C}$  NMR data for residue **E** (vide supra), it was concluded that a **B**(1→3)**E** linkage is present. On the **E** H-1 NOESY track, inter-residue cross-peaks were found with **D** H-3,4. Taking into account the methylation analysis/ $^{13}\text{C}$  NMR data for residue **D** (vide supra), the linkage was assigned as **E**(1→4)**D**. On the **D** H-1 track inter-residue NOESY connectivities were detected with **A**β H-3,4, and combined with the methylation analysis/ $^{13}\text{C}$  NMR data for residue **A**β (vide supra), a **D**(1→3)**A**β linkage was established. The observed intra-residue NOE cross-peaks were in accordance with the assigned anomeric configurations. The relevant long-range couplings in the  $^1\text{H}$ – $^{13}\text{C}$  HMBC spectrum confirmed the sequence established from the NOESY data (data not shown).

Combination of the structural information as presented above allowed structure **3** to be formulated as a linear pentasaccharide with the following sequence:



### 2.3. 2D NMR spectroscopy of the native polysaccharide

The complete assignment of the  $^1\text{H}$  and  $^{13}\text{C}$  chemical shifts of the native EPS (Table 2) was carried out by means of 2D TOCSY (mixing times, 40–200 ms), NOESY (mixing time, 150 ms), and  $^1\text{H}$ – $^{13}\text{C}$  HSQC experiments. The TOCSY spectrum (200 ms) of the EPS is shown in Figure 5, together with the NOESY spectrum. The  $^1\text{H}$ – $^{13}\text{C}$  HSQC spectrum is shown in Figure 6. Starting points for the interpretation of the spectra were the anomeric signals of residues **A**–**E**. Comparison of TOCSY spectra with increasing mixing times allowed the assignment of the sequential order of the chemical shifts belonging to the same spin system.

The TOCSY **A** H-1 track ( $\delta$  5.245) showed cross-peaks with **A** H-2,3,4, whereas on the **A** H-2 track the cross-peaks with **A** H-5,6a,b were found. The TOCSY **B** H-1 track ( $\delta$  5.165) revealed cross-peaks with **B** H-2,3,4,5,6a; via the **B** H-5 track the cross-peak with **B** H-6b was detected (confirmed by  $^1\text{H}$ – $^{13}\text{C}$  HSQC). On the TOCSY **C** H-1 track ( $\delta$  4.977) cross-peaks with **C** H-2,3,4,5,6a,6b were found. The TOCSY **D** H-1 track ( $\delta$  4.682) allowed the identification of the cross-peaks with **D** H-2,3,4,5 (confirmed by  $^1\text{H}$ – $^{13}\text{C}$  HSQC), whereas the **D** H-5 track revealed the resonances for **D** H-6a,6b. Finally, on the TOCSY **E** H-1 track ( $\delta$  4.537) cross-peaks with **E** H-2,3,4 were shown; the resonances for **E** H-5,6a,6b followed from  $^1\text{H}$ – $^{13}\text{C}$  HSQC experiments.

According to the assigned spin systems, with characteristic downfield chemical shifts for H-4, residues **B** and **E** were shown to have the *galacto*-configuration: residue **B** corresponds with  $\alpha$ -D-Galp and residue **E** with  $\beta$ -D-Galp (vide supra). The TOCSY results of residues **C** and **D** were in agreement with a *gluco*-configuration: Residue **C** corresponds to a terminal  $\alpha$ -D-Glcp unit (upfield chemical shift value of H-4), whereas residue **D** could be assigned as a  $\beta$ -D-Glcp residue (characteristic upfield shift of H-2).<sup>14</sup> Finally, taking into account the methylation analysis/ $^{13}\text{C}$  NMR data, residue **A** was assigned as a  $\beta$ -D-Galf unit.

Evaluation of the C-1 chemical shifts and the  $^1J_{\text{C-1,H-1}}$  coupling constants, deduced from 2D  $^1\text{H}$ – $^{13}\text{C}$  HMBC measurements, confirmed that residues **B** (Gal;  $\delta$  96.5; 173 Hz) and **C** (Glc;  $\delta$  99.0; 173 Hz) occur in  $\alpha$ -pyranosyl form, and residues **D** (Glc;  $\delta$  102.9; 163 Hz) and **E** (Gal,  $\delta$  103.9; 161 Hz) in  $\beta$ -pyranosyl form.<sup>12</sup> The  $^1J_{\text{C-1,H-1}}$  value for residue **A** (177 Hz) is indicative of a furanose ring, although it gives no information about the anomeric configuration of the residue.<sup>13</sup> However, a comparison of the C-1 chemical shift values of residue **A** ( $\delta$  110.5),  $\beta$ -D-Galf/1Me ( $\delta$  109.9), and  $\alpha$ -D-Galf/1Me ( $\delta$  103.8)<sup>13</sup> allowed the assignment of the  $\beta$ -configuration for residue **A**.

Taking into account published  $^{13}\text{C}$  chemical shift data of methyl aldoses,<sup>13</sup> and the methylation analysis data of the EPS, residue **A** was assigned as 3-substituted  $\beta$ -Galf (downfield shift of **A** C-3,  $\delta_{\text{C-3}}$  85.6;  $\beta$ -D-Galf/1Me,  $\delta_{\text{C-3}}$  78.4). In addition, residue **B** was assigned as 3,6-disubstituted  $\alpha$ -Galp (downfield shift of **B** C-3,  $\delta_{\text{C-3}}$  78.0; downfield shift of **B** C-6,  $\delta_{\text{C-6}}$  67.0;  $\alpha$ -D-Galp/1Me,  $\delta_{\text{C-3}}$  70.5,  $\delta_{\text{C-6}}$  62.2), residue **C** as terminal  $\alpha$ -Glcp, residue **D** as 4-substituted  $\beta$ -Glcp (downfield shift of **D** C-4,  $\delta$  79.4;  $\beta$ -D-Glcp/1Me,  $\delta_{\text{C-4}}$  70.6), and residue **E** as 3-substituted  $\beta$ -Galp (downfield shift of **E** C-3,  $\delta_{\text{C-3}}$  78.3;  $\beta$ -D-Galp/1Me,  $\delta_{\text{C-3}}$  73.8).

The determination of the sequence of the monosaccharide residues within the repeating unit of the EPS could be achieved through the assignment of the inter-residue cross-peaks in the 2D NOESY spectrum (Fig. 5) and the relevant long-range couplings in the HMBC spectrum (Table 3). Inspection of the NOESY spectrum showed on the **C** H-1 track an NOE connectivity with **B** H-6b, suggesting a **C**(1→6)**B** linkage. The inter-residue NOE cross-peaks between **B** H-1 and **E** H-3,4 gave evidence for a linkage between **B** and **E**. Considering the methylation analysis/ $^{13}\text{C}$  NMR data for residue **E** (vide supra), a **B**(1→3)**E** linkage is indicated. The observed NOESY cross-peak between **E** H-1 and **D** H-4 supported an **E**(1→4)**D** linkage. Furthermore, the **D** H-1, **A** H-2,3 NOESY connectivities, together with the methylation analysis/ $^{13}\text{C}$  NMR data for residue **A** (vide supra), established the **D**(1→3)**A** linkage. Finally, from the NOESY cross-peaks between residues **A** H-1 and **B** H-3,4, and taking into account the



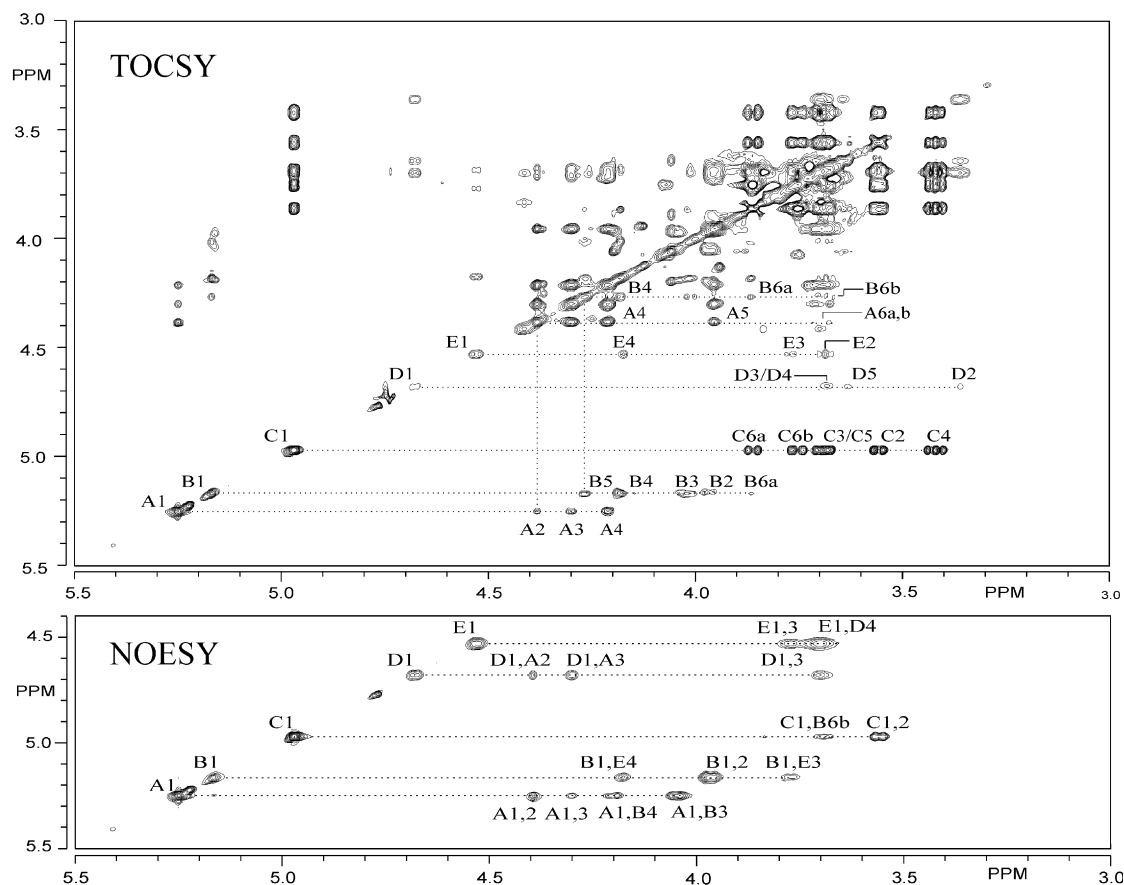


**Figure 5.** 2D TOCSY (mixing time, 200 ms) and NOESY (mixing time, 150 ms) spectra of EPS, recorded in D<sub>2</sub>O at 27 °C. Cross-peaks belonging to the same scalar-coupling network are indicated near a dotted line starting from the corresponding diagonal peaks; TOCSY: A1 corresponds to the diagonal peak of residue A H-1; A2 refers to a cross-peak between A H-1 and A H-2, etc.; NOESY: A1 corresponds to the diagonal peak of residue A H-1; A1,2 refers to an intra-residue cross-peak between A H-1 and A H-2, and A1,B3 indicates an inter-residue connectivity between A H-1 and B H-3, etc.

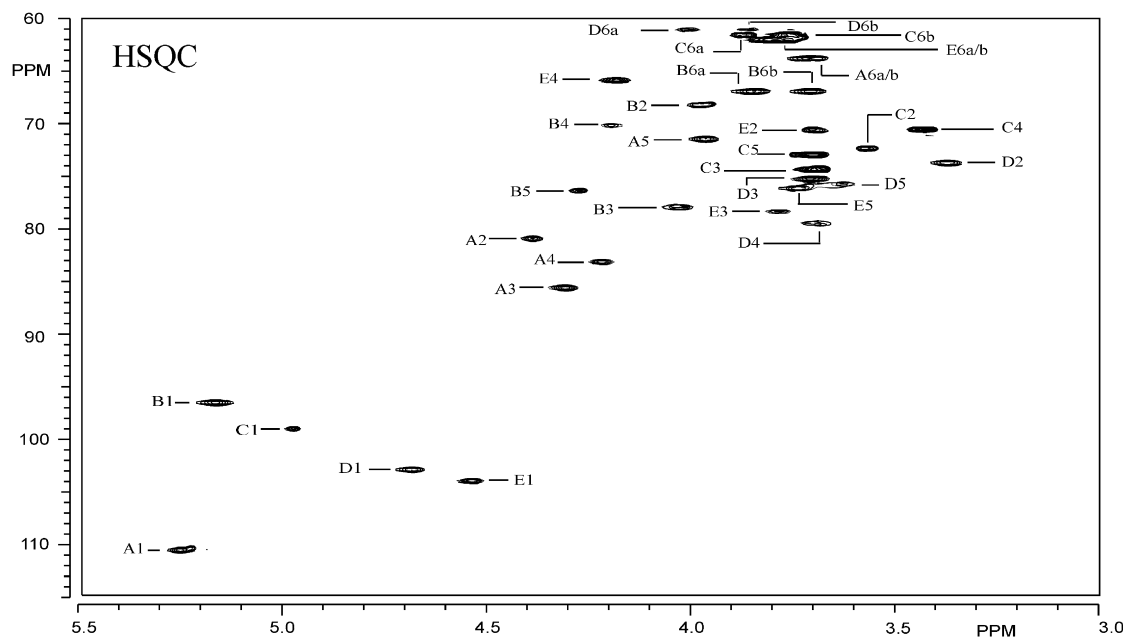


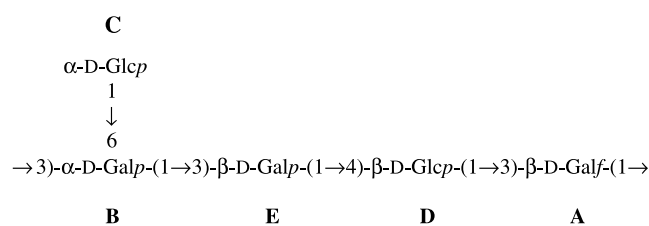
**Figure 6.** 2D <sup>1</sup>H–<sup>13</sup>C HSQC spectrum of EPS, recorded in D<sub>2</sub>O at 27 °C. A1 corresponds to the cross-peak between A H-1 and A C-1, etc.

**Table 3.** Long-range  $^1\text{H}$ – $^{13}\text{C}$  couplings found in the HMBC spectrum for the anomeric signals of the residues of EPS

Residue	$\delta_{\text{H-1/C-1}}$	Connectivities	Residue
<b>A</b>	5.245	85.6	<b>A</b> C-3
		83.2	<b>A</b> C-4
		78.0	<b>B</b> C-3
		4.06	<b>B</b> H-3
<b>B</b>	5.165	78.0	<b>B</b> C-3
		3.79	<b>E</b> H-3
<b>C</b>	4.977	74.4	<b>C</b> C-3
		72.9	<b>C</b> C-5
		67.0	<b>B</b> C-6
		3.84	<b>B</b> H-6a
<b>D</b>	4.682	85.6	<b>A</b> C-3
		4.31	<b>A</b> H-3
<b>E</b>	4.537	79.4	<b>D</b> C-4
		3.71	<b>D</b> H-4

methylation analysis/ $^{13}\text{C}$  NMR data for residue **B** (vide supra), the **A**(1→3)**B** linkage was identified. This confirmed residue **B** to be the branching point of the pentasaccharide repeating unit of the polysaccharide. The absence of inter-residue NOE cross-peaks involving signals of residue **C** other than CH-1, confirmed the identification of **C** as the only component of the side chain. The observed intra-residue NOE cross-peaks were in accordance with the assigned anomeric configurations.

Combining the various data of the EPS analysis, supported by the structural determination of the generated pentasaccharide fragment, shows that the polysaccharide is composed of the following pentasaccharide repeating unit:



The finding of a repeating unit as the major product in the partial acid hydrolysis of the EPS is in accordance with the known lability of a Galp-(1→*x*) linkage. Critical evaluation of the monosaccharide analysis of the EPS (the Glc content seems to be somewhat lower than 2), its methylation analysis (the peak ratio suggests a somewhat too high content of 3-substituted and a somewhat too low content of 3,6-disubstituted Galp), and its 1D  $^1\text{H}$  NMR peak pattern (additional small signals in the anomeric region), may suggest that some underglucosylation (5%) of the main chain, yielding a linear structure, is present.

## 2.4. Final remarks

Galactofuranosyl residues have been found together with galactopyranosyl residues in the structures of some EPSs produced by lactic acid bacteria, like *Lb. helveticus* TN-4 and Lh59,<sup>15,16</sup> *Lb. helveticus* 766,<sup>17</sup> *Lb. rhamnosus* C83,<sup>18</sup> KL37C,<sup>19</sup> and GG,<sup>20</sup> *Streptococcus macedonicus* Sc136,<sup>21</sup> *S. thermophilus* Sf39,<sup>22</sup> S3,<sup>23</sup> EU20,<sup>24</sup> SY89,<sup>25</sup> and SY102.<sup>25</sup> The coexistence of the furanosyl and pyranosyl residues suggests that these bacteria must have a mechanism for converting the pyranose into the furanose form.<sup>26</sup> However, none of the structures of the EPSs produced by *Lb. delbrueckii* ssp. *bulgaricus* reported so far contain galactofuranosyl residues.

## 3. Experimental

### 3.1. Production, isolation, and purification of the exopolysaccharide

The *Lb. delbrueckii* ssp. *bulgaricus* LBB.B26 strain, isolated from home-made yoghurt, was obtained from the LBB collection of LB Bulgaricum Plc. (Sofia, Bulgaria). An aliquot of an activated bacterial culture was used to inoculate 1 L of sterile (121 °C, 7 min) reconstituted skimmed milk powder in water (10% w/v; E. Merck, Darmstadt, Germany), and the strain was grown for 24 h at 42 °C. After incubation, proteins were removed from the culture medium by adding 80% (w/v) trichloroacetic acid (150 mL/L) and subsequent centrifugation at 10,000g for 10 min. After discarding the pellet, the EPS in the supernatant was precipitated with 3 vol of abs EtOH overnight at −18 °C, and collected by centrifugation at 10,000g for 10 min. A soln of the pellet in 40 mL hot distilled water (90 °C) was extensively dialyzed for 72 h against distilled water at 4 °C, then lyophilized. The freeze-dried sample was redissolved in 50 mM sodium phosphate buffer, pH 6.0, and an aliquot (1 mL; 3–10 mg of carbohydrate) was applied to a C16/20 column (Pharmacia Biotech, Uppsala, Sweden), packed with the weakly basic anion exchanger DEAE-Trisacryl Plus M (Sigma Aldrich Chemie GmbH, Taufkirchen, Germany). The neutral EPS was eluted with 50 mM sodium phosphate buffer, pH 6.0 (40 mL), at a flow rate of 0.5 mL/min, monitored at 280 nm with a UV-1 detector (Pharmacia Fine Chemicals, Uppsala, Sweden). The fractions containing the neutral EPS were pooled, desalted by dialysis against distilled water for 48 h at 4 °C, and lyophilized.

### 3.2. Molecular mass determination

The average molecular mass of the EPS was determined by gel filtration chromatography on a Sephacryl S-400 HR C16/100 column (Amersham Pharmacia Biotech,



Uppsala, Sweden), calibrated with dextran standards (Mw 1800, 750, 410, 150, 50, and 25 kDa; Fluka Chemie GmbH, Buchs, Switzerland), using 50 mM phosphate buffer, pH 6.0, containing 150 mM NaCl as eluent. The flow rate was 0.2 mL/min and the fraction size was 2 mL. The carbohydrate content of each fraction was determined by the phenol/sulfuric acid assay.<sup>27</sup>

### 3.3. Monosaccharide analysis

Oligo/polysaccharide was subjected to methanolysis (methanolic 1 M HCl; 18 h, 85 °C). The resulting mixtures of methyl glycosides were trimethylsilylated (1:1:5 hexamethyldisilazane–trimethylchlorosilane–pyridine; 30 min, room temperature), then quantitatively analyzed by GLC as described.<sup>28</sup> In addition, the absolute configurations of the monosaccharides were determined by GLC analysis of the trimethylsilylated (–)-2-butyl glycosides.<sup>29,30</sup> For both analyses, the identities of the monosaccharides were confirmed by gas–liquid chromatography/mass spectrometry (GLC–MS).<sup>28</sup>

### 3.4. Methylation analysis

Samples (native EPS or oligosaccharide) were permethylated using methyl iodide and solid sodium hydroxide in dimethyl sulfoxide as described previously.<sup>31</sup> After hydrolysis with 2 M TFA (2 h, 120 °C), the partially methylated monosaccharides were reduced with NaBD<sub>4</sub>. Conventional work-up, comprising neutralization and removal of boric acid by co-evaporation with methanol, followed by acetylation with 1:1 pyridine–acetic anhydride (30 min, 120 °C) yielded mixtures of partially methylated alditol acetates, which were analyzed by GLC–MS.<sup>28</sup>

### 3.5. Gas–liquid chromatography and mass spectrometry

Quantitative GLC analyses were performed on a Chrompack CP9002 gas chromatograph, equipped with an EC-1 column (30 m × 0.32 mm, Alltech, Deerfield, IL) using a temperature program of 140–240 °C at 4 °C/min and flame-ionization detection. GLC–MS analyses were carried out on a GC8060/MD800 system (Fisons instruments, Interscience; 70 eV), using an AT-1 column (30 m × 0.25 mm, Alltech) at the same temperature program.<sup>28</sup>

Matrix-assisted laser desorption ionization time-of-flight mass spectrometry (MALDI-TOF-MS) experiments were performed using a Voyager-DE PRO mass spectrometer (Applied Biosystems, Foster City, CA) equipped with a nitrogen laser (337 nm, 3 ns pulse width). Positive-ion mode spectra were recorded using the reflectron mode and delayed extraction (100 ns). The accelerating voltage was 20 kV with a grid voltage of 75.2%; the mirror voltage ratio was 1.12, and the acquisition mass range 500–3000 Da. Samples were pre-

pared by mixing on the target 1 µL oligosaccharide soln with 1 µL 2,5-dihydroxybenzoic acid (10 mg/mL) in 50% aq MeCN as matrix soln.

### 3.6. Partial acid hydrolysis

The polysaccharide (50 mg) was treated with 0.2 M trifluoroacetic acid (25 mL) for 1 h at 100 °C. The progress of the hydrolysis was checked by TLC (E. Merck Kieselgel 60 F254 sheets; 2:1:1 *n*-butanol–acetic acid–water; orcinol-sulfuric acid staining). After lyophilization, the residue was fractionated on a Bio-Gel P-4 column (90 × 1.5 cm), eluted with 10 mM NH<sub>4</sub>HCO<sub>3</sub> at a flow rate of 3 mL/min at room temperature, monitored by differential refraction index detection (LKB Bromma 2142 Differential Refractometer). The collected fractions were lyophilized and subjected to analysis.

### 3.7. NMR spectroscopy

Resolution-enhanced 1D/2D 500-MHz NMR spectra were recorded in D<sub>2</sub>O on a Bruker DRX-500 spectrometer (Bijvoet Center, Department of NMR Spectroscopy) at a probe temperature of 27 °C for oligosaccharides and polysaccharides. Prior to analysis, samples were exchanged twice in D<sub>2</sub>O (99.9 at % D, Cambridge Isotope Laboratories, Inc., Andover, MA) with intermediate lyophilization, and then dissolved in 0.6 mL D<sub>2</sub>O. Chemical shifts are expressed in ppm by reference to internal acetone ( $\delta$  2.225) for <sup>1</sup>H and/or to the  $\alpha$ -anomeric signal of external [1-<sup>13</sup>C]glucose ( $\delta_{C-1}$  92.9) for <sup>13</sup>C. Suppression of the HOD signal was achieved by applying a WEFT pulse sequence for 1D experiments<sup>32</sup> and by a pre-saturation of 1 s during the relaxation delay for 2D experiments.<sup>33</sup> 2D TOCSY spectra were recorded using an MLEV-17 mixing sequence<sup>34</sup> with spin-lock times of 40–200 ms. 2D NOESY experiments were performed with a mixing time of 150 ms for the polysaccharide and 1 s for the oligosaccharide. Natural abundance 2D <sup>1</sup>H–<sup>13</sup>C HSQC and HMBC experiments were recorded with and without decoupling, respectively, during acquisition of the <sup>1</sup>H FID. Resolution enhancement of the spectra was performed by a Lorentzian-to-Gaussian transformation or by multiplication with a squared-bell function phase shifted by  $\pi/(2.3)$  for 2D spectra, and when necessary, a fifth-order polynomial baseline correction was performed. All NMR data were processed using in-house developed software (J.A. van Kuik, Bijvoet Center, Utrecht University).

### Acknowledgements

The authors thank Dr. Bas R. Leeftang for help in the NMR measurements.

## References

1. De Vuyst, L.; Degeest, B. *FEMS Microbiol. Rev.* **1999**, *23*, 153–177.
2. Laws, A. P.; Gu, Y.; Marshall, V. M. *Biotechnol. Adv.* **2001**, *19*, 597–625.
3. Cerning, J.; Bouillanne, C.; Desmazeaud, M. J.; Landon, M. *Biotechnol. Lett.* **1988**, *10*, 255–260.
4. Uemura, J.; Itoh, T.; Kaneko, T.; Noda, K. *Milchwissenschaft* **1998**, *53*, 443–446.
5. Grobbsen, G. J.; van Casteren, W. H. M.; Schols, H. A.; Oosterveld, A.; Sala, G.; Smith, M. R.; Sikkema, J.; de Bont, J. A. M. *Appl. Microbiol. Biotechnol.* **1997**, *48*, 516–521.
6. Faber, E. J.; Kamerling, J. P.; Vliegthart, J. F. G. *Carbohydr. Res.* **2001**, *331*, 183–194.
7. Harding, L. P.; Marshall, V. M.; Hernandez, Y.; Gu, Y.; Maqsood, M.; McLay, N.; Laws, A. P. *Carbohydr. Res.* **2005**, *340*, 1107–1111.
8. Cerning, J.; Bouillanne, C.; Desmazeaud, M. J.; Landon, M. *Biotechnol. Lett.* **1986**, *8*, 625–628.
9. Grobbsen, G. J.; Sikkema, J.; Smith, M. R.; de Bont, J. A. M. *J. Appl. Bacteriol.* **1995**, *79*, 103–107.
10. Gruter, M.; Leeftang, B. R.; Kuiper, J.; Kamerling, J. P.; Vliegthart, J. F. G. *Carbohydr. Res.* **1993**, *239*, 209–226.
11. Harding, L. P.; Marshall, V. M.; Elvin, M.; Gu, Y.; Laws, A. P. *Carbohydr. Res.* **2003**, *338*, 61–67.
12. Bock, K.; Pedersen, C. *J. Chem. Soc., Perkin Trans. 2* **1974**, 293–297.
13. Bock, K.; Pedersen, C. *Adv. Carbohydr. Chem. Biochem.* **1983**, *41*, 27–66.
14. Robijn, G. W.; van den Berg, D. J. C.; Haas, H.; Kamerling, J. P.; Vliegthart, J. F. G. *Carbohydr. Res.* **1995**, *276*, 117–136.
15. Yamamoto, Y.; Nunome, T.; Yamauchi, R.; Kato, K.; Sone, Y. *Carbohydr. Res.* **1995**, *275*, 319–332.
16. Stinge, F.; Lemoine, J.; Neeser, J.-R. *Carbohydr. Res.* **1997**, *302*, 197–202.
17. Robijn, G. W.; Thomas, J. R.; Haas, H.; van den Berg, D. J. C.; Kamerling, J. P.; Vliegthart, J. F. G. *Carbohydr. Res.* **1995**, *276*, 137–154.
18. Vanhaverbeke, C.; Bosso, C.; Colin-Morel, P.; Gey, C.; Gamar-Nourani, L.; Blondeau, K.; Simonet, J.-M.; Heyraud, A. *Carbohydr. Res.* **1998**, *314*, 211–220.
19. Lipiński, T.; Jones, C.; Lemerminier, X.; Korzeniowska-Kowal, A.; Strus, M.; Rybka, J.; Gamian, A.; Heczko, P. B. *Carbohydr. Res.* **2003**, *338*, 605–609.
20. Landersjö, C.; Yang, Z.; Huttunen, E.; Widmalm, G. *Biomacromolecules* **2002**, *3*, 880–884.
21. Vincent, S. J. F.; Faber, E. J.; Neeser, J.-R.; Stinge, F.; Kamerling, J. P. *Glycobiology* **2001**, *11*, 131–139.
22. Lemoine, J.; Chirat, F.; Wieruszski, J.-M.; Strecker, G.; Favre, N.; Neeser, J.-R. *Appl. Environ. Microbiol.* **1997**, *63*, 3512–3518.
23. Faber, E. J.; van den Haak, M. J.; Kamerling, J. P.; Vliegthart, J. F. G. *Carbohydr. Res.* **2001**, *331*, 173–182.
24. Marshall, V. M.; Dunn, H.; Elvin, M.; McLay, N.; Gu, Y.; Laws, A. P. *Carbohydr. Res.* **2001**, *331*, 413–422.
25. Marshall, V. M.; Laws, A. P.; Gu, Y.; Levander, F.; Rådström, P.; de Vuyst, L.; Degeest, B.; Vaningelgem, F.; Dunn, H.; Elvin, M. *Let. Appl. Microbiol.* **2001**, *32*, 433–437.
26. Sutherland, I. W. *Biotechnology of Microbial Exopolysaccharides*; Cambridge University Press: Cambridge, 1990.
27. Dubois, M.; Gilles, K. A.; Hamilton, J. K.; Rebers, P. A.; Smith, F. *Anal. Chem.* **1956**, *28*, 350–356.
28. Kamerling, J. P.; Vliegthart, J. F. G. Carbohydrates. In *Clinical Biochemistry—Principles, Methods, Applications, Vol. 1, Mass Spectrometry*; Lawson, A. M., Ed.; Walter de Gruyter: Berlin, 1989; pp 175–263.
29. Gerwig, G. J.; Kamerling, J. P.; Vliegthart, J. F. G. *Carbohydr. Res.* **1978**, *62*, 349–357.
30. Gerwig, G. J.; Kamerling, J. P.; Vliegthart, J. F. G. *Carbohydr. Res.* **1979**, *77*, 1–7.
31. Ciucanu, I.; Kerek, F. *Carbohydr. Res.* **1984**, *131*, 209–217.
32. Hård, K.; van Zadelhoff, G.; Moonen, P.; Kamerling, J. P.; Vliegthart, J. F. G. *Eur. J. Biochem.* **1992**, *209*, 895–915.
33. Hård, K.; Vliegthart, J. F. G. In *Glycobiology, A Practical Approach*; Fukuda, M., Kobata, A., Eds.; Oxford University Press: Oxford, 1993; pp 223–242.
34. Bax, A.; Davis, D. G. *J. Magn. Reson.* **1985**, *65*, 355–360.